PCCP

PAPER

View Article Online
View Journal | View Issue

Cite this: *Phys. Chem. Chem. Phys.*, 2014, **16**, 11310

Analysis of hydrogen bond energies and hydrogen bonded networks in water clusters $(H_2O)_{20}$ and $(H_2O)_{25}$ using the charge-transfer and dispersion terms

Suehiro Iwata

Received 20th March 2014,
Accepted 16th April 2014

DOI: 10.1039/c4cp01204f

www.rsc.org/pccp

The hydrogen bonds and their networks in the water clusters $(H_2O)_{20}$ and $(H_2O)_{25}$ are characterized using the charge-transfer $\left(E_{CT}^{W_a,W_d}\right)$ and dispersion $\left(E_{Disp}^{W_a,W_d}\right)$ terms for every pair of water molecules (W_a, W_d) in the clusters. The terms are evaluated by the perturbation theory based on the *ab initio* locally projected molecular orbitals (LPMO PT) developed by the present author. The relative binding energies among the isomers evaluated by the LPMO PT agree with those of the high level *ab initio* wave function based theories. A strong correlation between $E_{CT}^{W_a,W_d}$ and $E_{Disp}^{W_a,W_d}$ for the hydrogen bonded pairs is found. The pair-wise interaction energies are characterized by the types of hydrogen-donor (W_d) and hydrogen-acceptor (W_a) water molecules. The strongest pair is that of the D2A1 water molecule as a hydrogen-acceptor and the D1A2 water molecule as a hydrogen-donor, where the D*n*A*m* water molecule implies that the water molecule has *n* hydrogen bonding O–H and *m* accepting H···O. The intra-molecular deformation as well as the O···O distance is also dependent on the types of hydrogen bonded pairs. The ring structures in the cluster are classified by the pattern of alignment of the hydrogen bonds. The lengthening of the hydrogen-bonding OH of W_d is strongly correlated with the charge-transfer $\left(E_{CT}^{W_a,W_d}\right)$ energy.

1 Introduction

The properties of hydrogen bonded networks in water clusters have been extensively studied both experimentally and theoretically. Xantheas and his coworkers reported a series of high level computational studies on finite sizes of water clusters, and they recently reviewed the work.[1] The stable isomers of water clusters $(H_2O)_n$, $n \geq 3$, contain the ring (cyclic) structures of the hydrogen bonded networks. The isomers of $(H_2O)_n$, n = 17–21, reported by Lagutchenkov, Fanourgakis and Xantheas consist of 4-membered and 5-membered rings,[2] but they do not have 6-membered rings. On the other hand, all of the isomers of $(H_2O)_{25}$ reported by Furtado *et al.* have 6-membered rings, and one of them has a 7-membered ring.[3] It is well-known that the 6-membered ring structures are the main units of various phases of water assemblies, such as liquid water, amorphous water and crystal ice. In the finite sizes of stable water clusters, the 6-membered ring structures start to appear around $n \sim 24$. Because every water molecule has two donating OH bonds and two O···H-accepting sites, even a single 6-membered ring $(H_2O)_6$ has several distinct isomers of different alignments of the hydrogen bonded molecules. McDonald *et al.*[4] counted the 30 026 distinct isomers of the dodecahedron $(H_2O)_{20}$, which differ by the direction of the hydrogen bonds. Kirov reported that the number of symmetry-distinct configurations emanating from the different hydrogen positions is 3 043 836 for $5^{12}6^2$ T-cage $(H_2O)_{24}$ and 61 753 344 for $5^{12}6^4$ H-cage $(H_2O)_{28}$.[5,6]

In the last decade the author has been developing the *ab initio* molecular orbital theory suitable for the study of the weak molecular interaction.[7–10] The most important target systems of these studies are the hydrogen bonded clusters, in particular, of water clusters. In most of the *ab initio* computations of the non-covalent weak molecular clusters, using both wave function based and density functional theories, the supermolecular approach is commonly used. The computations can be carried out straightforwardly without the intuitive division of the target systems. The interaction energy is evaluated as the difference of large numbers. Because the interaction energy is much smaller than the total electron energy of the system, the well-balanced approximation for the separated systems and for the assembled system becomes important. Because of the inconsistent approximation for the one-electron functions (molecular orbitals) and for the many-electron functions (electron configuration), the

Department of Chemistry, Faculty of Science and Technology, Keio University, Hiyoshi, Yokohama 223-8522, Japan. E-mail: iwatasuehiro@gmail.com

basis set superposition error (BSSE) sneaks in the binding energy. To avoid the BSSE, there are several attempts. Our approach is to use the local basis sets for the molecular orbitals of each component molecule. The method is called the Locally Projected Molecular Orbital (LPMO) perturbation theory (PT), and several applications are published.[7–10] One of the advantages of the method is that the charge-transfer and dispersion terms between each pair of molecules can be directly evaluated from the first order perturbation wave function.

In the previous papers,[11,12] using the charge-transfer terms between the hydrogen bonded pairs, we classified the water molecules by D*n*A*m*, where *n* is the number of hydrogen-donor OHs and *m* is the number of H atoms accepted by the molecule. The hydrogen bonds were characterized by D*n*A*m* ← D*n*′A*m*′, D*n*A*m* (D*n*′A*m*′) being the hydrogen acceptor (donor) water molecule. Similar characterization is proposed by various papers. Ohno *et al.*[13] also classified the pair of hydrogen bonded water molecules using the calculated harmonic frequency shifts and compared the observed vibrational spectra of water clusters. Xantheas[14] defined (da), (aa), (dd), (da) and (aad) for each water cluster in the local hydrogen bonded network of $n \leq 6$. Singer and his coworkers introduced the graph invariants for the water clusters,[4,15] and the second order graph invariants were used to fit the empirical binding energy. They noted that the energies of these isomers are dependent on the number of the nearest-neighbor pairs of double acceptor water clusters in the clathrate structure.[15]

The present work is the extension of the previous studies[11,12] of larger water clusters which have more ring structures in the clusters.

2 Theoretical and computational procedure

2.1 The binding energy and its analysis

A series of our papers documented the theoretical basis and the procedure to evaluate the binding energy and its terms in the perturbation theory based on the locally projected molecular orbitals (LPMO PT).[9–11,16] Here, we describe the basic equations that pertain to the following discussion.[12] In LPMO, the zero order wave function Ψ^{LPMO} for a molecular cluster is a single Slater determinant constructed from sets of local MOs. These MOs are canonical for each molecule but not for the whole cluster, and therefore, the first order wave function starts with the single excitations as

$$\Psi^{1\mathrm{ST}} = \sum_{\mathrm{Mol=X}}^{\mathrm{X}} |\mathrm{LE_X}\rangle + \sum_{\mathrm{Mol=X,Y}}^{\mathrm{X}\neq\mathrm{Y}} |\mathrm{CT_{X\rightarrow Y}}\rangle + \sum_{\mathrm{Mol=X,Y}}^{\mathrm{X}<\mathrm{Y}} |\mathrm{Disp_{X-Y}}\rangle \tag{1}$$

where $|\mathrm{LE_X}\rangle$ stands for the single excitations within molecule X, and $|\mathrm{CT_{X\rightarrow Y}}\rangle$ stands for the single excitations from molecules X to Y, whereas $|\mathrm{Disp_{X-Y}}\rangle$ stands for the double excitations of the dispersion type. This expansion is made possible by defining the locally projected excited MOs, most of which are expanded in terms of the basis sets on each molecule X.[7] Because of the orthogonality condition to the occupied MOs of the other molecules {Y}, the coefficient vectors of some of the excited MOs of molecule X have to be partially delocalized over the basis sets on the other molecules {Y}. This restricted expansion can avoid the basis set superposition error (BSSE) caused both by the orbital basis inconsistency (OBI) and by the configuration basis inconsistency (CBI).[9,16]

The calculated binding energy in this approximation can be written as

$$E_{\mathrm{BindE}}^{\mathrm{3SPT+Disp}} \equiv \left(E_{\mathrm{HF}}(\Psi_{\mathrm{LPMO}}) - \sum_{\mathrm{X}} E_{\mathrm{HF}}^{\mathrm{X}}\right) + \left(E^{\mathrm{2SPT}} + E^{\mathrm{3SPT}}\right) + E^{\mathrm{2DPT\_Disp}} \tag{2}$$

$$\equiv E_{\mathrm{BindE}}^{\mathrm{LPMO}} + E_{\mathrm{CT+LE}}^{\mathrm{2\&3SPT}} + E_{\mathrm{Disp}} \tag{3}$$

$$\equiv E_{\mathrm{BindE}}^{\mathrm{LPMO-2\&3SPT}} + E_{\mathrm{Disp}} \tag{4}$$

The first parentheses in eqn (2) represent the binding energy $E_{\mathrm{BindE}}^{\mathrm{LPMO}}$ evaluated by LPMO, which contains the electrostatic, exchange-repulsion and induction (polarization) terms as well as the destabilization energy caused by the geometric deformation. The second parentheses in eqn (2) are the second and third order corrections of the single excitations $E_{\mathrm{CT+LE}}^{\mathrm{2\&3SPT}}$, and is evaluated by the sum

$$E_{\mathrm{CT+LE}}^{\mathrm{2\&3SPT}} = \sum_{\mathrm{Mol=X,Y}}^{\mathrm{X}<\mathrm{Y}} \left(E_{\mathrm{CT}}^{\mathrm{X\leftarrow Y}} + E_{\mathrm{CT}}^{\mathrm{Y\leftarrow X}}\right) + \sum_{\mathrm{Mol=X}} E_{\mathrm{LE}}^{\mathrm{X}} \tag{5}$$

in which the contribution from the local excitations $E_{\mathrm{LE}}^{\mathrm{X}}$ is non-zero only at the third order and is always much smaller than the charge-transfer terms. Because the terms in eqn (5) are calculated using the first order wave function (1), each term is directly tabulated for any clusters consisting of any number of molecules when the sum $E_{\mathrm{CT+LE}}^{\mathrm{2\&3SPT}}$ is evaluated. This is contrasted with the ALMO-EDA (absolutely local MO – energy decomposition analysis) of Head-Gordon's group, in which the CT energy is defined by the difference between the total energies of the HF (or Kohn–Sham DFT) determined using the full basis sets and using the ALMO.[17,18] The Slater determinant of ALMO is equivalent to the zero order wave function Ψ^{LPMO} of our LPMO PT. The ALMO-EDA cannot separate the CT terms to each pair of the molecules when the interacting system consists of more than two molecules. The charge-transfer energy is very much definition-dependent, and therefore, the absolute values have to be used in the analysis with care. The dispersion terms are better defined than the charge-transfer terms because they result from the electron correlation of the inter-molecules. But for the molecular interaction where the orbital overlaps between molecules are significant, the distinction of the intra- and inter-molecule electron correlation becomes unclear.

We demonstrated for several types of molecular interaction that, if the aug-cc-pVxZ type basis sets[19] are used, the binding energy $E_{\mathrm{BindE}}^{\mathrm{LPMO-2\&3SPT}}$ evaluated using the third order single excitation wave function approximates the counterpoise (CP) corrected Hartree–Fock energy $E_{\mathrm{BindE}}^{\mathrm{CPcorrected\ HF}}$.[9,10] Thus, $E_{\mathrm{BindE}}^{\mathrm{3SPT+Disp}}$ in eqn (4) is the "approximate BSSE-free HF + dispersion" energy.

2.2 Computational details

The in-house *ab initio* MO program, MOLYX, was partially parallelized for the present study using OpenMP. The new revision enabled us to compute the energy, $E_{\mathrm{BindE}}^{\mathrm{3SPT+Disp}}$, of $(H_2O)_{25}$ with the aug-cc-pVDZ set on the SGI UV2000 at the RCCS, Okazaki Research facilities of National Institutes of Natural Science (NINS). The load modules, compiled by the intel compiler using MKL, are available both for Mac OS X and for Linux on request.

The geometries of most of the water clusters are those reported by Xantheas and his coworkers, and they are reviewed in a recent article,[1] and are cited in the previous paper.[12] They are optimized with MP2/aug-cc-pVDZ. The geometries of the isomers of $(H_2O)_{17}$, $(H_2O)_{18}$, $(H_2O)_{19}$ and $(H_2O)_{20}$ are those reported by Xantheas and his coworkers.[2,20] More recently Xantheas extended the search of the low-lying isomers and the global minima of $(H_2O)_{20}$,[24] and compared the energies of many isomers of the pentagonal dodecahedron. In addition, for $(H_2O)_{20}$, six isomers determined by Gadre and his coworkers are also studied.[3] To find the isomers, they made combined use of the temperature basin paving (TBA) procedure[21] and the molecular tailoring approach (MTA).[22,23] Six isomers of $(H_2O)_{25}$ similarly determined by them[3] are also studied.

The charge-transfer term $E_{\mathrm{CT}}^{\mathrm{X,Y}}(\equiv E_{\mathrm{CT}}^{\mathrm{X}\leftarrow\mathrm{Y}} + E_{\mathrm{CT}}^{\mathrm{Y}\leftarrow\mathrm{X}} + E_{\mathrm{LE}}^{\mathrm{X}} + E_{\mathrm{LE}}^{\mathrm{Y}})$ for the pair of the hydrogen bonded water molecules (X, Y) is used to identify the hydrogen bond and its direction. Subsequently the hydrogen bonding matrix, defined by Miyake and Aida,[25] is set up. By manipulating the matrix, the water molecules and the hydrogen bonds are classified, and then the *r*-membered ring structures in the clusters are identified.

3 Results and discussion

3.1 Relative binding energy of $(H_2O)_{20}$ and $(H_2O)_{25}$

Tables 1 and 2 compare the relative binding energy of $(H_2O)_{20}$ and $(H_2O)_{25}$. Because the optimization procedures of ref. 2 and 3 slightly differed from each other, the energies of two groups of isomers of $(H_2O)_{20}$ are compared separately. The most stable isomers of two groups, an edge-sharing pentagon prism in the former and G20E in the latter, share the "almost" same geometric structure (The difference is described below). As is seen in tables, the LPMO PT results agree well with the MP2 energies (Note that the energy unit is kJ mol^{-1}). A similar agreement was found for $(H_2O)_6$, $(H_2O)_{11}$ and $(H_2O)_{16}$ in the previous work.[12] In general, the relative energies of $E_{\mathrm{BindE}}^{\mathrm{3SPT+Disp}}$/aug-cc-pVDZ are close to those of MP2/aug-cc-pVTZ. It is because HF/aug-cc-pVTZ is also nearly BSSE-free as $E_{\mathrm{BindE}}^{\mathrm{3SPT}}$ is. The total binding energies ($E_{\mathrm{BindE}}^{\mathrm{3SPT+Disp}}$/aug-cc-pVDZ) are -853.3 kJ mol^{-1} for the prism edge-sharing isomer of $(H_2O)_{20}$, and -1071.0 kJ mol^{-1} for the G25D isomer of $(H_2O)_{25}$. The average hydrogen bonding energy is -25.1 kJ mol^{-1} for the former, and -25.5 kJ mol^{-1} for the latter. The largest discrepancy of $E_{\mathrm{BindE}}^{\mathrm{3SPT+Disp}}$ from the MP2 energies is found for isomer G25D, which is a unique isomer having a 7-membered ring and no 6-membered rings. As shown in Fig. 1, the other isomers of $(H_2O)_{25}$ studied in the present paper have 6-membered rings.

Table 1 Comparison of the relative binding energy (kJ mol^{-1}) of the isomers of $(H_2O)_{20}$

Isomers	$E_{\mathrm{BindE}}^{\mathrm{3SPT+Disp}}$ eqn (4)	MP2	MP2	MTA–MP2[a]	MTA–MP2[a]	MTA–MP2[a]	$\mathbf{R}_4$; $\mathbf{R}_5$[e]
Ref. 2	apVDZ[b]	apVDZ[b]	apVTZ[b]	CBS[d]	apVTZ[b]	apVDZ[b]	
Edge-sharing	0.0	0.0	0.0				$(4)^5(31)^4(1111)^3;(5)^1(41)^3(32)^2$
Fused-cube	6.2	7.4(9.0)[c]	(10.5)[c]				$(4)^{13}(1111)^8$
Face-sharing	6.5	4.9(5.8)	(7.9)				$(4)^6(31)^3(1111)^6;(5)^4$
Dodecahedron	47.6	52.3(53.5)	(46.7)				$(5)^4(41)^5(32)^1(2111)^1$
Ref. 3							
G20E $\simeq$ edge-sharing	0.0	0.0		0.0	0.0	0.0	$(4)^4(31)^5(1111)^3;(5)^2(41)^2(32)^2$
G20A	10.5	7.1		2.1	6.7	6.3	$(4)^2(1111)^4;(5)^4(41)^6$
G20B	6.4	6.7		10.9	5.9	9.2	$(31)^3(1111)^1;(5)^4(41)^4(32)^3(2111)^2$
G20C	8.0	7.2		7.5	7.5	7.5	$(4)^5(31)^5(1111)^4;(5)^2(41)^2$
G20D	14.2	14.8		15.5	15.5	15.5	$(4)^3(31)^9(22)^2;(5)^1(41)^1(32)^2$
G20F	10.5	10.0		10.5	11.3	10.9	$(4)^4(31)^9(22)^3;(5)^1(41)^1(32)^2$

[a] Ref. 3. [b] apVXZ = aug-cc-pVXZ. [c] Ref. 2. [d] The two-point extrapolation to complete basis set. [e] See text for definition.

Table 2 Comparison of the relative binding energy (kJ mol^{-1}) of the isomers of $(H_2O)_{25}$

Isomers	$E_{\mathrm{BindE}}^{\mathrm{3SPT+Disp}}$ eqn (4)	MP2	MTA–MP2[a]	MTA–MP2[a]	MTA–MP2[a]	$\mathbf{R}_4$; $\mathbf{R}_5$; $\mathbf{R}_6$; $\mathbf{R}_7$[d]
Ref. 3	apVDZ[b]	apVDZ[b]	CBS[c]	apVTZ[b]	apVDZ[b]	
G25A	0.0	0.0	0.0	0.0	0.0	$(4)^1(31)^4;(5)^5(41)^9(32)^1(2111)^2;(33)^1$
G25B	-3.1	3.0	0.8	2.1	4.2	$(4)^2(31)^3(1111)^1;(5)^4(41)^2(32)^7(2111)^2;(6)^1(51)^1(42)^1$
G25C	1.9	4.1	1.3	2.5	5.4	$(4)^2(31)^2(1111)^2;(5)^5(41)^8(2111)^2;(6)^1(51)^3(3111)^1$
G25D	-8.7	4.5	2.1	2.9	5.0	$(4)^3(31)^3(1111)^2;(5)^2(41)^4(32)^2(2111)^2;(61)^1$
G25E	-2.2	3.7	2.9	3.4	4.2	$(4)^1(31)^3(1111)^2;(5)^3(41)^8(32)^2(2111)^2;(6)^1(51)^1(42)^1$
G25F	-0.5	9.4	6.3	7.5	10.0	$(4)^2(31)^4;(5)^4(41)^6(32)^3(2111)^2;(51)^2(33)^1$

[a] Ref. 3. [b] apVXZ = aug-cc-pVXZ. [c] The two-point extrapolation to complete basis set. [d] See text for definition.

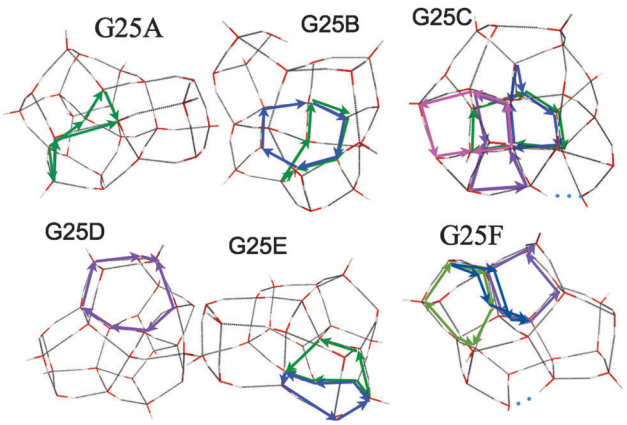

Fig. 1 Schematic structures and hydrogen-bonded networks of $(H_2O)_{25}$. The arrowed chains show the 6- and 7-membered rings. The color figures, which can be seen in the online version, show the 6- and 7-membered rings connected with the arrows.

Here we have to recall the fact that there are numerous isomers which have the exactly same topological configuration of the oxygen atoms in the water clusters.[4] Using the empirical potential functions, Kuo *et al.*[15] evaluated the binding energies of these 30 026 isomers of the pentagonal dodecahedron $(H_2O)_{20}$, and the energy difference of the maximum and minimum isomers is more than 130 kJ mol^{-1} in their empirical potential. Tokmachev *et al.*[26] also reported the binding energy of all of 30 026 isomers using the other empirical potential, and their maximum and minimum difference is 148 kJ mol^{-1}. Chihaia *et al.*[27] also studied the dodecahedron $(H_2O)_{20}$ isomers using the *ab initio* HF and DFT. By selecting six isomers of the dodecahedron $(H_2O)_{20}$ using the empirical total dipole moment as a measure, they optimized the isomers using HF/6-311G*, and evaluated the binding energy using B3LYP/6-311++G** without the BSSE correction. Their calculated energies range from −1149 to −880 kJ mol^{-1} with B3LYP/6-311++G** and from −950 to −712 kJ mol^{-1} with HF/6-311G*.[27] In the present study only one dodecahedron isomer was calculated, and is shown in Table 1, this dodecahedron isomer is the least stable among the ten isomers studied. This isomer is not necessarily the most stable among the 30 026 distinct isomers of the dodecahedron. Because Xantheas and his coworkers performed the extensive sampling of the isomers using TIP4P potential, the dodecahedron isomer they obtained is expected to be one of the most stable isomers. Recently Xantheas extended the computational studies of the pentagonal dodecahedron $(H_2O)_{20}$ isomers,[24] and compared the binding energies of the lowest 20 isomers obtained using various empirical potentials and the DFT and MP2 calculations.

As was reported by Xantheas and his coworkers,[2,20] and as is also seen in Table 1, the other isomers of $(H_2O)_{20}$ are more stable than the dodecahedron. The number of hydrogen bonds in the cluster, which is given in the second column of Table 3, is the smallest for dodecahedron isomers (30) among the isomers studied. But it is not the number of hydrogen bonds that determines the order of the stability. Fig. 2 shows the terms in eqn (3) and (4). The dispersion term (the rightmost column for each isomer) of the dodecahedron isomer is distinctly smaller than that of the other isomers. Similarly in $(H_2O)_6$, the dispersion term for the cyclic-chair isomer is much smaller than that for the other isomers such as cage and prism forms of the isomers.[11,28] Without the dispersion term, the cyclic isomer is the most stable. Because of the long-range nature of the dispersion interaction, the substantial dispersion terms are found between the non-neighboring water molecules in the cage and prism isomers of $(H_2O)_6$.[11] The dispersion interaction between non-neighboring molecules in the more compact forms of the isomers of $(H_2O)_{20}$ contributes to the total binding energy. The dodecahedron isomer studied in this work has other characteristics; the largest E_{CT} and the smallest E_{BindE}^{LPMO}; the latter contains the deformation energy caused by forming

Table 3 Some characteristic indices of the isomers of $(H_2O)_{20}$ and $(H_2O)_{25}$

Isomers	HB[a]	$[N_{D1A2}, N_{D2A1}, N_{D2A2}]$[b]	D2A1 ← D1A2[c]	D2A2 ← D2A2[c]	D1A2 ← D2A1[c]	r^{n_r}, r = 4–7[d]
Edge-sharing	34	[6, 6, 8]	6	2	6	4^{12}, 5^6
Fused-cube	36	[4, 4, 12]	4	20	4	4^{21}
Face-sharing	35	[5, 5, 10]	6	2	6	4^{15}, 5^4
Dodecahedron	30	[10, 10, 0]	17	0	7	5^{12}
G20E ≃ edge-sharing	34	[6, 6, 8]	6	10	6	4^{12}, 5^6
G20A	32	[7, 7, 5]	10	4	6	4^6, 5^{10}
G20B	33	[7, 7, 6]	7	6	7	4^4, 5^{14}
G20C	34	[6, 6, 8]	8	10	4	4^{14}, 5^4
G20D	34	[6, 6, 8]	9	12	5	4^{14}, 5^4
G20F	34	[6, 6, 8]	7	10	5	4^{14}, 5^4
G25A	42	[8, 8, 9]	6	10	6	4^5, 5^7, 6^1
G25B	42	[8, 8, 9]	10	4	6	4^6, 5^{15}, 6^3
G25C	42	[8, 8, 9]	7	6	7	4^6, 5^{14}, 6^4
G25D	42	[8, 8, 9]	8	10	4	4^8, 5^{11}, 7^1
G25E	42	[8, 8, 9]	9	12	5	4^6, 5^{15}, 6^3
G25F	42	[8, 8, 9]	7	10	5	4^6, 5^{15}, 6^3

[a] The number of hydrogen bonds in the cluster. [b] N_{DnAm}: the number of water molecules of D*n*A*m* type. [c] The number of hydrogen bonds between the hydrogen acceptor D*n*A*m* and the hydrogen donor D*n*′A*m*′. [d] r^{n_r}: the number of *r*-membered rings in the cluster.

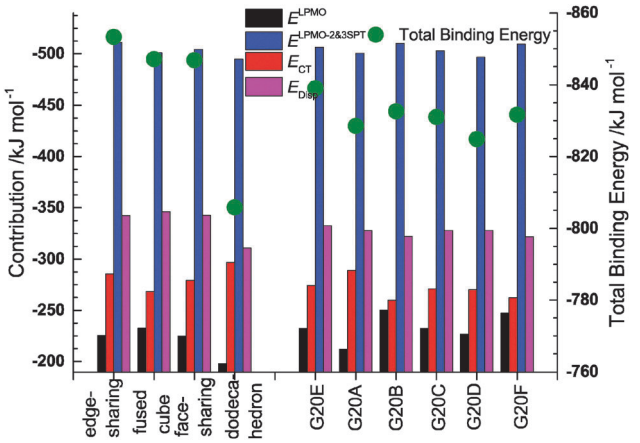

Fig. 2 Energy analysis of the isomers of $(H_2O)_{20}$. ●: the total binding energy $E_{BindE}^{3SPT+Disp}$ (Note that the right ordinate and its scale differ from those of the left ordinate for the columns). The first of four columns for each isomer is the first term, E_{BindE}^{LPMO}, of eqn (3). The second column is the second term, $E_{CT+LE}^{2\&3SPT}$, of eqn (3). The third is the sum of these two terms, $E_{BindE}^{LPMO-2\&3SPT}$, and is the first term of eqn (4). The last column is the dispersion term, E_{Disp}.

the strict regular pentagons. The two terms are inter-related to each other; the water molecules are deformed to favor the CT interaction in twelve 5-membered rings of the dodecahedron configuration.

In Table 3, the number of water molecules N_{DnAm} and the number of hydrogen bonded pairs DnAm ← Dn'Am' are given. They take various values both for $(H_2O)_{20}$ and $(H_2O)_{25}$. The number of dangling bonds of these clusters is equal to N_{D1A2}. The last column of Table 3 shows the number of r-membered ring structures $\{n_r, r = 4–7\}$ as r^{n_r}. The dodecahedron $(H_2O)_{20}$ has twelve 5-membered rings, while the edge-sharing prism isomer $(H_2O)_{20}$ has twelve 4-membered rings and six 5-membered rings. While counting the number of 6-membered rings, a little care is needed; when two neighboring 6-membered rings share four water molecules, there is another 6-membered ring. The examples are found in isomers G25B and G25E.

The r-membered rings are classified by the directions of the hydrogen bond chains in the ring. For instance, for the 4-membered hydrogen bonded rings, there are three ways of forming the rings of water clusters:

(4): $W_1 \leftarrow W_2 \leftarrow W_3 \leftarrow W_4 \leftarrow W_1$
(31): $W_1 \leftarrow W_2 \leftarrow W_3 \rightarrow W_4 \leftarrow W_1$
(1111): $W_1 \leftarrow W_2 \rightarrow W_3 \leftarrow W_4 \rightarrow W_1$

The index $\mathbf{R}_r$ in the last column of Tables 1 and 2 shows the numbers of the ring types in the network. For example, $\mathbf{R}_4$ of the edge-sharing prism isomer is $(4)^5(31)^4(1111)^3$, which implies that there are five 4-membered rings of type (4), four 4-membered rings of type (31) and three 4-membered rings of type (1111). The geometric structure of the isomer G20E of Gadre's group is almost identical with that of the edge-sharing prism except that $\mathbf{R}_4$ of G20E is $(4)^4(31)^5(1111)^3$. The types of ring structure in $\mathbf{R}_r$ are closely related to the stability of the clusters. The geometric characteristics of 20 isomers of the pentagonal dodecahedron $(H_2O)_{20}$ isomers studied by Xantheas are not described in the paper.[24] It should be examined how the relative binding energy of these isomers is related to the index $\mathbf{R}_5$. More systematic computations for large clusters are required to derive some general rules for the stability of the ring types in the clusters. In smaller cyclic isomers of $(H_2O)_r$, r = 3–6, the most stable cyclic isomers have the hydrogen bonded chain, aligned to the same direction as type (r) in the above definition. Inside of the large clusters, as seen in Fig. 1, the rings are nested to each other. Therefore, not all of the hydrogen bonds are able to align in the same direction for some of the rings.

Interestingly, all of the isomers of $(H_2O)_{25}$ of Gadre's[3] have the same number of hydrogen bonds, N_{D1A2}, N_{D2A1}, and N_{D2A2}, even though, without any guiding principle for finding the stable configurations, the optimization started from the structures determined by the temperature basin paving (TBA) procedure.[21] As Fig. 1 and the last column of Tables 2 and 3 show, however, the hydrogen bonded networks in these isomers are very different from each other. Their total binding energies are close to each other (within 10 kJ mol^{-1}). It seems that TBA of Shanker and Bandyopadhyay is an efficient procedure to find many candidates of the stable conformers as they claimed.[21]

3.2 Analysis of hydrogen bond energies

Fig. 3 shows the plots of the charge-transfer $E_{CT}^{X,Y}$ and dispersion terms $E_{Disp}^{X,Y}$ as a function of the the O···O length for every pair of hydrogen bonds in $(H_2O)_{17}$ ~ $(H_2O)_{21}$. The different symbols are used for the types of pair of hydrogen-acceptor and hydrogen-donor water molecules. The strongest type of the hydrogen bonds is D2A1 ← D1A2 (an upper-ward triangle mark), and almost all of the short O···O distance (≤2.7 Å) hydrogen bonds are of this type. The strong correlation between $E_{CT}^{X,Y}$ and $E_{Disp}^{X,Y}$ can be noticed, in

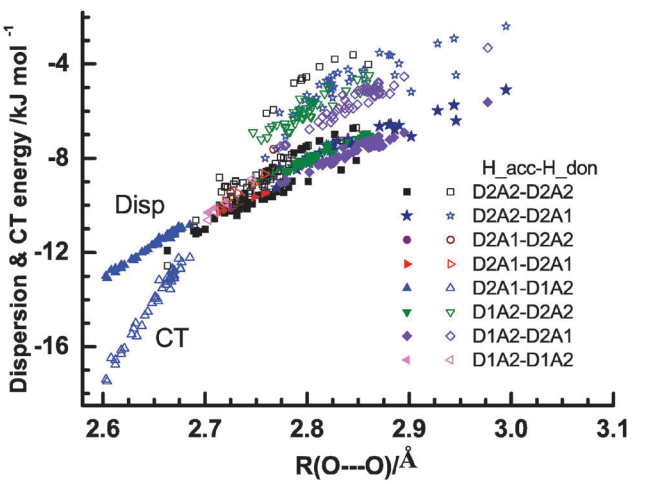

Fig. 3 Correlation of the O···O length with the charge-transfer $E_{CT}^{X,Y}$ and dispersion $E_{Disp}^{X,Y}$ energy for the isomers of $(H_2O)_{17}$ ~ $(H_2O)_{21}$ optimized by Xantheas and his coworkers.[2,20] Different symbols are used, depending on the types of the pair of hydrogen-acceptor and hydrogen-donor water clusters. The filled points are for $E_{Disp}^{X,Y}$.

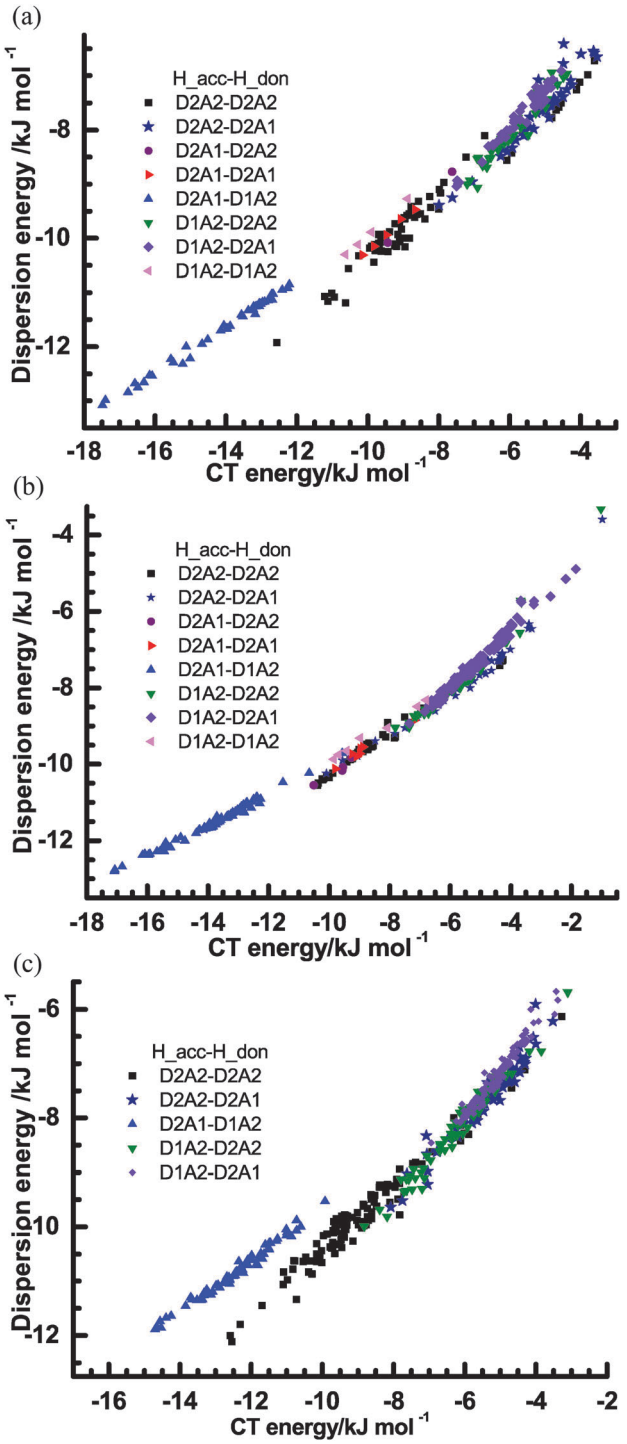

Fig. 4 Correlation between charge-transfer $E_{CT}^{X,Y}$ and dispersion $E_{Disp}^{X,Y}$ terms, classified by the types of the hydrogen bonded pairs. (a) The isomers of $(H_2O)_{17} \sim (H_2O)_{21}$ optimized by Xantheas and his coworkers.[2] (b) The isomers of $(H_2O)_n$, n = 2–16 optimized by Xantheas and his coworkers.[20] (c) The isomers of $(H_2O)_{20}$ and $(H_2O)_{25}$ optimized by Gadre and his coworkers.[3]

particular, for this type of hydrogen bond. This correlation is more clear in Fig. 4, in which the direct correlation between $E_{CT}^{X,Y}$ and $E_{Disp}^{X,Y}$ is shown (a) for $(H_2O)_{17}$ – $(H_2O)_{21}$, (b) for $(H_2O)_n$, $2 \leq n \leq 16$,[2,20] and (c) for $(H_2O)_{20}$ and $(H_2O)_{25}$.[3] The next strongest pair is D2A2 ← D2A2 (a square mark). The bonds of D1A2 ← D1A2 (a left-ward triangle) and D1A2 ← D2A2 (a downward triangle) have an intermediate strength. The pairs D2A2 ← D2A1 (a star mark) and D1A2 ← D2A1 (a rhombus) are weaker than the other types. Except for the D2A2 ← D2A2 hydrogen bonds, when the D2 water molecules are the hydrogen-donors, the hydrogen bonds are relatively weak in general. This leads to an important consequence for the stability of the ring structure. For instance, if index $\mathbf{R}_r$ is (1111) for a 4-membered ring, (2111) for a 5-membered ring, or (3111) for a 6-membered ring, there are two D2 water molecules in the ring. If these D2 molecules are not hydrogen-bonded from the molecules outside of the ring to become D2A2, both water molecules form relatively weak hydrogen bonds. The last column of Tables 1 and 2 shows that most of the isomers have these indices. The fused-cube isomer of $(H_2O)_{20}$ has eight (1111) 4-membered rings. By changing the direction of the hydrogen bonds in these rings, more stable fused-cube isomers than that studied might be found. The dodecahedron isomer studied has only one (2111) 5-membered ring, which suggests that this might be one of the most stable rings among the 30 026 dodecahedrons.

Fig. 4b shows that in smaller clusters the strong D2A1 ← D1A2 (a upper-ward triangle mark) and weak D1A2 ← D2A1 (a rhombus mark) bonds are dominant. They together often make the chained forms in the cluster. The D2A2 ← D2A2 bonds in this figure are mostly of isomers $(H_2O)_{16}$.[12] As seen in Table 3 and Fig. 4c, there are many D2A2 ← D2A2 hydrogen bonds in $(H_2O)_{20}$ and $(H_2O)_{25}$, and they contribute to the stability of the clusters. The approximate linear relationship of $E_{CT}^{X,Y}$ and $E_{Disp}^{X,Y}$ for this type of bond can be noticed in Fig. 4. Also it should be emphasized that the dispersion term is dominant in the D2A2 ← D2A2 hydrogen bonds, which are the bonds that construct the hydrogen bonded networks in large water clusters as well as in liquid water and ice. Fig. 3 and 4 demonstrate that the interaction energies and the O···O lengths depend on the pair of the hydrogen-donor and -acceptor water molecules, but that their values are distributed in broad ranges; the neighboring hydrogen bonds influence the hydrogen bonds electronically and by the structural constraints. The non-additive and many-body effects, which are not fully accounted for in the classification by the type of the hydrogen bonded pairs DnAm ← Dn'Am', cause a certain distribution of the plots in figures.

Fig. 4c for $(H_2O)_{20}$ and $(H_2O)_{25}$ of Gadre's group more clearly shows that the relationship between $E_{CT}^{X,Y}$ and $E_{Disp}^{X,Y}$ in the D2A1 ← D1A2 bonds is different from that in the other types of hydrogen bonded pairs. The dispersion terms for the D2A1 ← D1A2 bonds are smaller than those for the D2A2 ← D2A2 bonds. Because the D1A2 water molecule has a dangling bond, the molecule is at the surface of the cluster. Fig. 5 shows the dependence of $E_{CT}^{X,Y}$ and O–H_b on the O···O length in the isomers of $(H_2O)_{20}$ and $(H_2O)_{25}$,[3] where H_b is the hydrogen bonding hydrogen. The plots clearly show the lengthening of O–H bonds by the hydrogen bond formation. This lengthening is related to the well-known experimental and theoretical observations in the low-frequency shifts of the harmonic

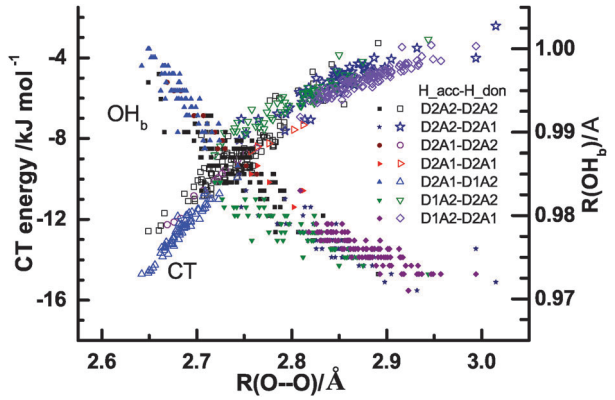

Fig. 5 Correlation of the O···O distance with the charge-transfer energy $E_{CT}^{X,Y}$ and O–H_b for the isomers of $(H_2O)_{20}$ and $(H_2O)_{25}$,[3] where H_b is the hydrogen bonding hydrogen. The unfilled points are for $E_{CT}^{X,Y}$.

frequency of the OH stretching modes.[13] The lengthening of O–H_b is positively correlated with $E_{CT}^{X,Y}$, and depends on the types of hydrogen bonds.

Fig. 6 shows the plots of the OH lengths of the water molecules. The abscissa is the sum $\sum_{Y\neq X} E_{CT}^{Y\leftarrow X}$ of molecule X

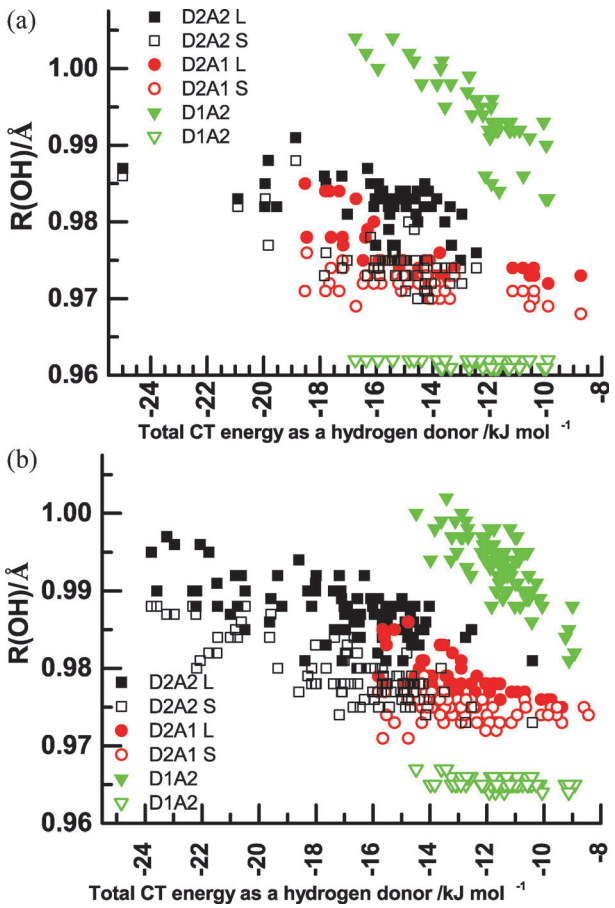

Fig. 6 Relationship of the O–H distance of a hydrogen donor water molecule X with the sum $\sum_{Y\neq X} E_{CT}^{Y\leftarrow X}$. The unfilled marks are for the shorter OH bonds of D2 water molecules. (a) $(H_2O)_{17}$ ~ $(H_2O)_{21}$[2] and (b) $(H_2O)_{20}$ and $(H_2O)_{25}$.[3]

of D*n*A*m* type. When X is the D1 type of water, a single term dominates in the sum $\sum_{Y\neq X} E_{CT}^{Y\leftarrow X}$. The large value of the sum (left-ward at the abscissa) implies that water X is a good hydrogen donor and electron acceptor. Understandably the length of the dangling OH (unfilled down-ward triangles) of the D1A2 water is independent of the sum (the abscissa). It can be noticed that these lengths of the dangling OH in Fig. 6(a) and (b) are slightly different by about 0.002 Å. It is because the geometries come from the different sources.[2,3] The hydrogen bonding OH (filled down-ward triangles) of D1A2 water is substantially lengthened, and the weakening of the bond depends on the charge-transfer energy as the hydrogen donor, but the change is not linear. In a simple orbital theory of charge-transfer interaction, the σ* anti-bonding orbital of OH_b is an electron acceptor orbital. Both Fig. 6(a) and (b) clearly demonstrate the close correlation of the charge-transfer energy and the OH_b lengthening. The amount of charge-transfer, and, in other words, the weakening of the OH bond, are sensitive to the surrounding geometric constraints. The plots in Fig. 6 are not able to show the details of the causes. Figures show that both in D2A2 and D2A1 water molecules, two OH_b bonds are not equivalent in most of the cases; the longer one of each molecule is shown by the filled mark. In figures the square points of D2A2 and the circle points of D2A1 are located at the abscissa less than twice of those (down-ward triangles) of D1A2, which implies that the lengthening of the OH bonds is not a simple linear function of the charge-transfer interaction.

These plots are another demonstration that $E_{CT}^{X,Y}$ in the present definition is a good measure to characterize the strength of the hydrogen bonds and hydrogen bonded networks.

4 Concluding remarks

The work demonstrates that LPMO PT is a practical and reasonably accurate *ab initio* MO method to study the molecular interaction, and can be applied for a large size of water clusters without a big computer resource. Importantly the method provides us not only the binding energy but also the pair-wise interaction terms, which help to characterize the interaction energy pair-wisely. The water molecules in the water clusters are classified by D*n*A*m*, and the hydrogen bonds are characterized by the D*n*A*m* ← D*n*′A*m*′. The strongest hydrogen bonds are of the type D2A1 ← D1A2. Another significant finding is the close correlation of the OH_b lengthening and the charge-transfer energy. The *r*-membered rings in the water clusters are also classified by the lengths of the in-phase hydrogen bonds, and the numbers of these rings in the cluster are related to the stability of the cluster. As studied by Singer and his coworkers,[4] there are numerous numbers of isomers of $(H_2O)_n$ of the same topological configuration of the oxygen atoms, whose hydrogen bonded networks differ only in their directions. The present results provide some guidance for a systematic search of the isomers favored both in terms of energy and entropy, and help for further *ab initio* computations of the large clusters having many 6-membered rings.

Acknowledgements

The work is partially supported by the Grants-in-Aid for Science Research (No. 23550031) of JSPS. A part of computations was carried out at the RCCS, Okazaki Research Facilities, National Institutes of Natural Sciences (NINS). The author acknowledges Dr K. Ishimura for instructing him how to parallelize the code using OpenMP.

References

1 S. Yoo and S. S. Xantheas, in *Handbook of Computational Chemistry*, ed. J. Leszczynski, Springer, 2012, ch. Structures, Energetics, and Spectroscopic Fingerprints of Water Clusters n = 2–24, pp. 761–792.
2 A. Lagutchenkov, G. S. Fanourgakis and S. S. Xantheas, *J. Chem. Phys.*, 2005, **122**, 194310.
3 J. P. Furtado, A. P. Rahalkar, S. Shanke, P. Bandyopadhyay and S. R. Gadre, *J. Phys. Chem. Lett.*, 2012, **3**, 2254–2258.
4 S. McDonald, L. Ojamae and S. J. Singer, *J. Phys. Chem. A*, 1998, **102**, 2824–2832.
5 M. V. Kirov, *J. Struct. Chem.*, 2002, **43**, 790–797.
6 S. Yoo, M. V. Kirov and S. S. Xantheas, *J. Am. Chem. Soc.*, 2009, **131**, 7564–7566.
7 T. Nagata and S. Iwata, *J. Chem. Phys.*, 2004, **120**, 3555–3563.
8 S. Iwata, *Chem. Phys. Lett.*, 2006, **431**, 204–209.
9 S. Iwata, *J. Phys. Chem. B*, 2008, **112**, 16104–16109.
10 S. Iwata, *J. Chem. Phys.*, 2011, **135**, 094101.
11 S. Iwata, *Phys. Chem. Chem. Phys.*, 2012, **14**, 7787–7794.
12 S. Iwata, P. Bandyopadhyay and S. S. Xantheas, *J. Phys. Chem. A*, 2013, **117**, 6641–6651.
13 K. Ohno, M. Okimura, N. Akai and Y. Katsumoto, *Phys. Chem. Chem. Phys.*, 2005, **7**, 3005–3014.
14 S. S. Xantheas, *Chem. Phys.*, 2000, **258**, 225–231.
15 J.-L. Kuo, J. V. Coe, S. J. Singer, Y. B. Band and L. Ojamae, *J. Chem. Phys.*, 2001, **114**, 2527–2540.
16 S. Iwata, *J. Phys. Chem. A*, 2010, **114**, 8697–8704.
17 R. Z. Khaliullin, A. T. Bell and M. Head-Gordon, *J. Chem. Phys.*, 2008, **128**, 184112.
18 R. J. Azar and M. Head-Gordon, *J. Chem. Phys.*, 2012, **136**, 024103.
19 J. T. H. Dunning, *J. Chem. Phys.*, 1989, **90**, 1007–1023.
20 G. S. Fanourgakis, E. Apra and S. S. Xantheas, *J. Chem. Phys.*, 2004, **121**, 2655–2663.
21 S. Shanker and P. Bandyopadhyay, *J. Phys. Chem. A*, 2011, **115**, 11866–11875.
22 V. Ganesh, R. K. Dongare, P. Balanarayan and S. R. Gadre, *J. Chem. Phys.*, 2006, **125**, 104109–104118.
23 A. P. Rahalkar, V. Ganesh and S. R. Gadre, *J. Chem. Phys.*, 2009, **129**, 234101–234107.
24 S. S. Xantheas, *Can. J. Chem. Eng.*, 2012, **90**, 843–851.
25 T. Miyake and M. Aida, *Chem. Phys. Lett.*, 2006, **427**, 215–220.
26 A. M. Tokmachev, A. L. Tchougreeff and R. Dronskowski, *ChemPhysChem*, 2010, **11**, 384–388.
27 V. Chihaia, S. Adams and W. F. Kuhs, *Chem. Phys.*, 2004, **297**, 271–287.
28 F.-F. Wang, G. Jenness, W. A. Al-Saidi and K. D. Jordan, *J. Chem. Phys.*, 2010, **132**, 134303.